ISEIS

Journal of Environmental Informatics 35(1) 81-93 (2020)

Journal of Environmental Informatics

www.iseis.org/jei

Stochastic Evolutionary-Based Optimization for Rapid Diagnosis and Energy-Saving in Pilot- and Full-Scale Carrousel Oxidation Ditches

L. Li[1], L. Lei[1], M. S. Zheng[1], A. G. L. Borthwick[2], and J. R. Ni[1,*]

[1]*Department of Environmental Engineering, Peking University; Key Laboratory of Water and Sediment Sciences, Ministry of Education, Beijing 100871, China*
[2]*Institute of Energy Systems, School of Engineering, The University of Edinburgh, The King's Buildings, Edinburgh EH9 3JL, UK*

Received 13 April 2017; revised 3 June 2017; accepted 6 June 2017; published online 10 October 2017

ABSTRACT. Energy consumption is a primary issue needed to be considered for wastewater treatment targeting qualified effluent. In this paper, a hybrid model is proposed for rapid diagnosis of operational conditions meeting requirements of discharge standards and energy saving in the pilot- and full-scale Carrousel Oxidation Ditches (ODs). Based on a three-dimensional (3D) three-phase computational fluid dynamics (CFD) model, we developed an artificial neural network (ANN) model with back propagation algorithm and an accelerating genetic algorithm (AGA) model to achieve real-time simulation and system optimization in the Carrousel ODs. By incorporating the 3D-CFD and multi-site ANN models, the hybrid model provided reasonable predictions of liquid flow, sludge sedimentation and water quality in the Carrousel ODs. With help of the AGA model based on evolution theory, system optimization could be reached to meet multiple purposes such as energy saving, water-quality improving and normal sludge distribution, which was demonstrated that a 31% saving in total energy could possibly be made under an optimum operating condition compared to the existing operating condition in a full-scale OD.

Keywords: three-dimensional three-phase, artificial neural network, rapid feedback, optimization, energy saving, oxidation ditch

1. Introduction

As one of the modified activated sludge treatment processses (Zhou et al., 2015; Wei et al., 2016), oxidation ditches (ODs) are continuous loop reactors containing multi-channels. Surface aerators and rotating impellers in ODs provide circulation, mixing and uneven distribution of dissolved oxygen (DO) to remove contaminates (Jin et al., 2015). ODs are utilized worldwide because of their reliable removal efficiency, convenient management and low sludge production (EPA, 1992). However, there remain many challenges (Zhang et al., 2016), namely a typical OD occupies a large area of land, the deposition of sludge is usually uneven thereby reducing the effective area of the OD, and the OD equipment often consume a large amount of energy to ensure the effluent quality. Therefore, system optimization of ODs is of primary importance not only to meet the prescribed effluent quality standards but also to minimize operating costs.

Accurate understanding of the physical-chemical-biological processes in ODs is essential when determining equipment upgrades and optimized operating conditions to meet environmental and economic criteria. A growing number of mathematical models have been proposed to simulate multi-phase behavior and simultaneous nitrification and denitrification (SND) in OD systems. Of the most famous, activated sludge models (ASMs) proposed by the International Water Association (IWA) (Henze et al., 2000) are widely used to predict effluent water quality and biomass production of wastewater treatment plants. Subsequently, many models have been built to reflect the hydraulics, chemical and biological processes in ODs by coupling the computational fluid dynamics (CFD) model with ASMs (Glover et al., 2006; Littleton et al., 2007). More recently, a three-dimensional (3D) three-phase CFD model has been developed at Peking University, which produced reasonable simulations of liquid flow velocity and concentrations of DO, COD and nutrients that matched experimental data (Lei et al., 2014). Specially, this model represented activated sludge flocs as a pseudo-solid phase in order to characterize sludge transportation and gas/liquid-solid interactions within the OD. On the other hand, over 20 parameters were needed to model the floc feature and biological processes, and longer computational time was required to simulate one operational mode. Hence, further efforts are needed to achieve real-time simulation for in-time response to incidental events.

For fast prediction of the behaviors of all kinds of materials in ODs, a multi-layer artificial neural network (ANN)

* Corresponding author. Tel.: +(86)10-62751185; fax: +(86)10-62756526.
E-mail address: jinrenni@pku.edu.cn (J. R. Ni).

ISSN: 1726-2135 print/1684-8799 online
 doi: 10.3808/jei.201700377

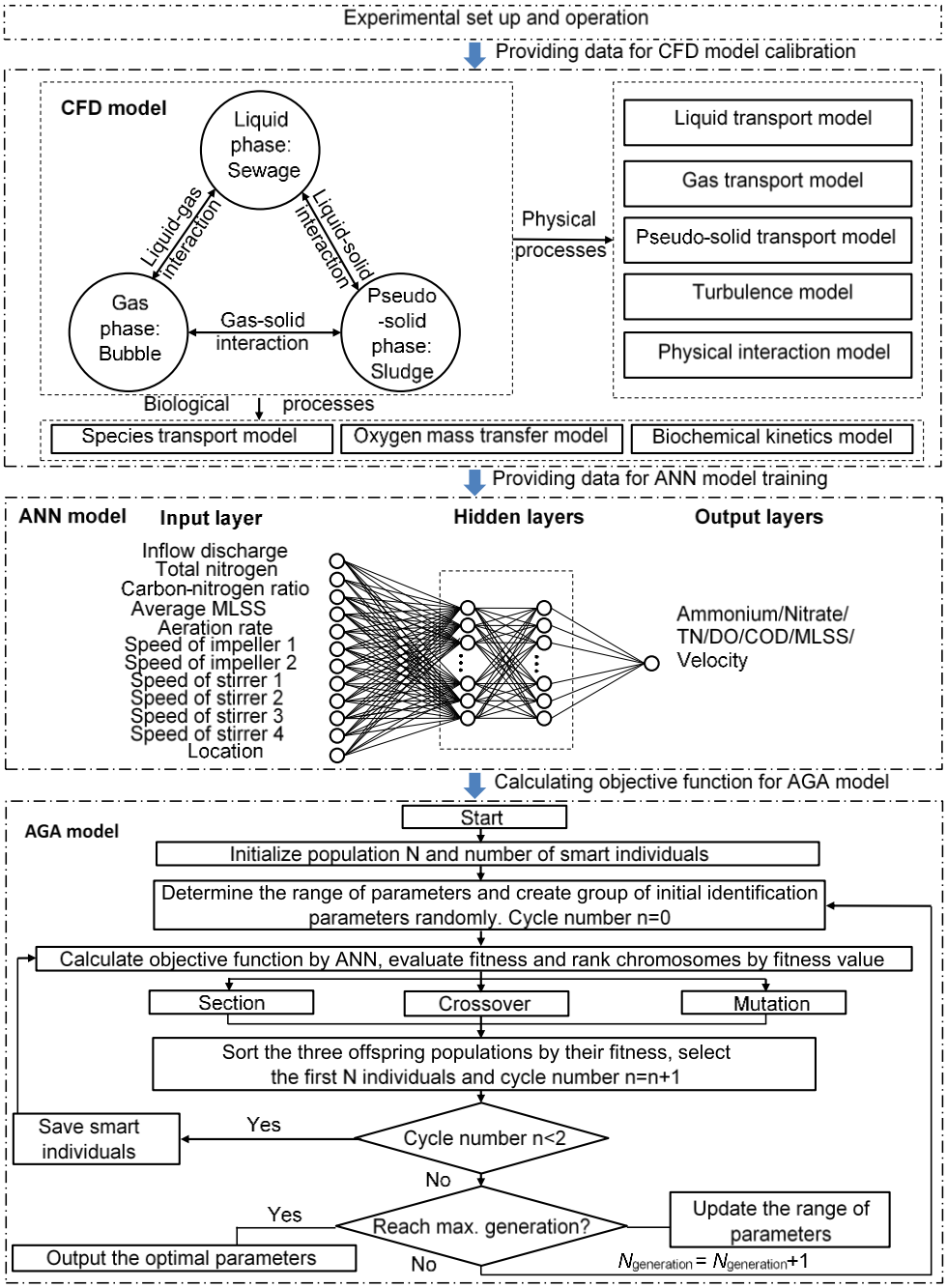

Figure 1. Framework of hybrid model of conditions in the oxidation ditch, comprising a three-dimensional (3D) three-phase computational fluid dynamics (CFD) model, multi-site artificial neural network (ANN) model and accelerating genetic algorithm (AGA) model.

with back propagation (BP) algorithm was introduced in combination with the CFD model. Only few inputs are required by the ANN model for effectively solving non-linear problems (Binetti et al., 2017; Fernando et al., 2017) and handling complicated systems (Purkait et al., 2008; Bahrami et al., 2016). To date, a substantial body of literature is available on the use of ANN in modeling wastewater treatment processes. Researchers have applied ANN to estimate wastewater process parameters (Häck et al., 1996), to develop control schemes (Zeng et al., 2003), and to predict the wastewater treatment performance of wastewater treatment plants (WWTPs) at laboratory scale, including anaerobic-anoxic-oxic system (Ma et al., 2011), sequencing batch reactor (Aguado et al., 2009) and submerged membrane bioreactor (Çinar, 2006). However, few efforts have been made in full-scale wastewater treatment processes due to diffi-

Table 1. Rotational Modes of Impellers and Stirrers

Moving part	Case I		Case II		Case III		Case IV	
	Speed (rpm)	Direction	Speed (rpm)	Direction	Speed (rpm)	Direction	Speed (rpm)	Direction
Impeller 1	40	+*	80	+	180	+	40	+
Impeller 2	40	+	80	+	180	+	40	+
Stirrer 1	40	–**	90	–	120	–	70	–
Stirrer 2	40	+	90	+	120	+	70	+
Stirrer 3	40	+	90	+	120	+	70	+
Stirrer 4	50	+	70	+	115	+	50	+

* + clockwise rotation. ** – anticlockwise rotation.

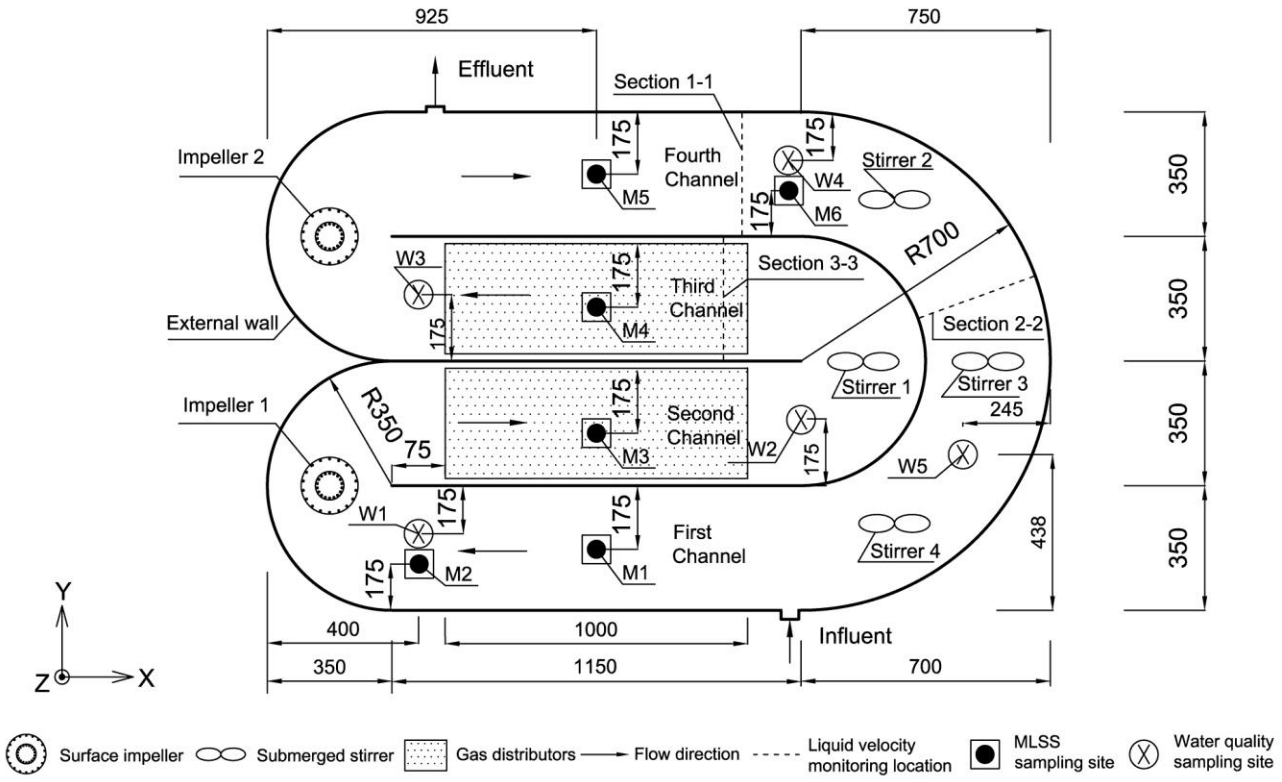

Figure 2. Schematic of pilot-scale oxidation ditch and monitoring sites (unit: mm).

culties in obtaining comprehensive data for model calibration and verification.

Since WWTPs are complex non-linear systems (Shen et al., 2008), their control and optimization are not easy to achieve. In practice, implementation of these tasks relies heavily on operator experience and empirical guidelines (Karpinska et al., 2016), both of which tend to be insufficiently detailed and subject to considerable uncertainty. As a result, model-based control approaches have been increasingly proposed with respect to different objectives like nitrate control (Stare et al., 2007) and DO control (Holenda et al., 2008). However, few control methods have considered sludge settlement. In an OD system, the uneven deposition of sludge reduces the effective area (He et al., 2014) and leads to malodorous septic sludge occurring in dead zones (Pipes, 1969). It is therefore necessary to evaluate sludge settling in order to achieve acceptable effluent standard at low operational cost.

In this paper, a hybrid model was established by incorporating CFD and ANN models to provide real-time feedback of the three phase flows by rapid simulation of the coupled physical-chemical-biological processes in the ODs, and a system optimization was enhanced by an inserted accelerating genetic algorithm (AGA). Figure 1 illustrates the model framework. Firstly, a 3D three-phase CFD model, validated by experimental results, was employed as a data engine to provide adequate information by which to train the ANN model. Next, a multi-site ANN model with BP algorithm was used to extract the outputs of the CFD model and to achieve real-time simulation in the ditch. Finally, an AGA model based on stochastic evolutionary theory was combined with the ANN model to determine the optimal condition to meet requirements of effluent quality, evenness of sludge distribution

and less energy consumption simultaneously. The hybrid model was demonstrated of great potential in practical applications in pilot- and full-scale Carrousel ODs.

2. Methodology

2.1. Experimental Set Up and Operation of the Pilot-Scale Oxidation Ditch

A pilot-scale Carrousel OD was fabricated with plexiglass with a total working volume of 1.40 m^3. The pilot OD consisted of four straight channels (1.15 m long, 0.35 m wide and 0.50 m still deep; Figure 2), the ends of each were joined by semi-circular connecting channels, small one of radius 0.35 m, the big one of radius 0.70 m. Two surface impellers (Impellers 1 and 2) and four submerged stirrers (Stirrers 1, 2, 3 and 4) were inserted in the semi-circular channels to drive the circulating flow in the reactor; the flow direction was indicated by arrows in Figure 2. Table 1 lists the rotational speeds and angular directions of the impellers and stirrers used in the CFD model (calibration: Case II; validation: Case IV) and ANN model (training and validation: Case I, II and III; test: Case IV). A series of 1- meter-long gas distributors controlled by the rotameter were located at the bottom of the second and third channels to supply air in the ditch, and hence form aerobic zones. Synthetic wastewater was stored in a tank of 1.8 m^3 total volume. The wastewater was composed of 1 m^3 tap water, 250 g sugar, 107.2 g NH_4Cl, 61.3 g $Na_3PO_4 \bullet 12H_2O$, 10 g $CaCl_2$, 3 g $FeSO_4 \bullet 7H_2O$, 500 g $NaHCO_3$, 12 g $MgSO_4$, and 50 mL trace element solution; this provided COD and NH_4^+-N concentrations of 250 mg/L and 50 mg/L, respectively. The synthetic wastewater was pumped into the OD at a flow rate of 0.1 m^3/h to guarantee a hydraulic retention time of 14 h; and 60 L of mixed liquor was discharged daily from the outlet of the ditch to maintain the sludge retention time of 25 d. A settling tank with a volume of 0.15 m^3 was used to separate the activeted sludge which was recycled to the ditch at a 100% sludge recycle ratio. During experiments, the temperature was maintained at 20 - 24 °C, and the pH was approximately 7.8. Twice weekly, the liquid velocity was monitored at the Section 1-1, 2-2 and 3-3, and the mixed liquor suspended solid (MLSS) was measured 0.1 m above the bed at locations M1, M2, M3, M4, M5 and M6. DO concentrations were recorded twice daily, 0.25 m above the bed at locations W1, W2, W3, outlet, W4 and W5. Water samples were also collected twice daily 0.25 m above the bed at W1, W2, W3, outlet, W4 and W5, for water quality analysis in order to monitor the concentrations of ammonia nitrogen, nitrate, total nitrogen (TN), and COD.

2.2. Three-Dimensional Three-Phase CFD Model

The 3D multi-phase hydrodynamics model for describing motion of wastewater, activated sludge and gas in the OD is based on the following continuity and momentum conservation equations:

$$\frac{\partial}{\partial t}(\alpha_q \rho_q) + \nabla \cdot (\alpha_q \rho_q \vec{v}_q) = \sum_{p=1}^{n} (m_{pq} - m_{qp}) + S_q \quad (1)$$

and

$$\begin{aligned} &\frac{\partial}{\partial t}(\alpha_q \rho_q \vec{v}_q) + \nabla \cdot (\alpha_q \rho_q \vec{v}_q \vec{v}_q) \\ &= -\alpha_q \nabla p + \nabla \cdot \tau_q + \alpha_q \rho_q \vec{g} \\ &\quad + \sum_{p=1}^{n} (\vec{R}_{pq} + m_{pq} \vec{v}_{pq} - m_{qp} \vec{v}_{qp}) \\ &\quad + (\vec{F}_q + \vec{F}_{lift,q} + \vec{F}_{vm,q}) \end{aligned} \quad (2)$$

where α_q is the volume fraction of the phase q, such that $\sum_{q=1}^{3} \alpha_q = 1$, ρ_q is the density of phase q, $\vec{v}_q$ is the velocity vector of phase q, S_q is the source term relating to the phase q, m_{pq} is the mass transfer from phase p to q, and the subscripts q = 1, 2 and 3 denote wastewater, gas and active sludge, respectively. p is the pressure shared by all phases, $\vec{g}$ is the vector of gravitational acceleration, $\vec{R}_{pq}$ is the interaction force vector between phases, $\vec{v}_{pq}$ is the interphase velocity vector, $m_{pq}\vec{v}_{pq} - m_{pq}\vec{v}_{pq}$ denotes the momentum change due to mass transfer between the phase p and q, $\vec{F}_q$ is the external body force, $\vec{F}_{lift,q}$ is the lift force, $\vec{F}_{vm,q}$ is the virtual mass force and τ_q is the q phase stress-strain tensor.

The advection-dispersion species transport equation was used to describe the growth, decay, and transformation of activated biomass (e.g. heterotrophs and autotrophs) and contaminants (e.g., soluble COD, ammonia nitrogen and nitrate) in the OD, and the source terms were included in the equation (Lei et al., 2014).

The rate of oxygen mass transfer from the gas to liquid phase is determined from:

$$\rho_3 = K_L a_L (\alpha S_{O(S)} - S_O) \quad (3)$$

in which $K_L a_L$ is the mass transfer coefficient, calculated as the sum of surface and bottom aeration. $S_{O(S)}$ is the saturated DO concentration in clean water, S_O is the oxygen concentration in the liquid phase, and α is a coefficient. For surface aeration, the mass transfer coefficient for sewage water is expressed as:

$$\begin{aligned} \frac{K_L a_L}{\sqrt{\varepsilon}} &= 0.64 exp(-0.29 e^{-0.98}) \\ &\quad + 1.6 \times 10^{-6} exp[0.72(e - 3.91)^2] \end{aligned} \quad (4)$$

where ε is the dissipation rate of the turbulent kinetic energy.

Using Gambit, an unstructured mesh containing 161,987 tetrahedra was created representing the OD geometry, and refined in the aerator and rotating zones (Figure 3). The equations were solved at steady state using the finite volume me-

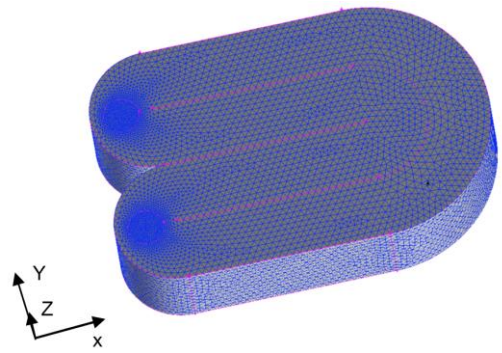

Figure 3. Grids of the computational domain in a pilot-scale oxidation ditch.

thod in Fluent 6.3. Open boundary conditions were set at the inlet and outlet of the ditch. At the inlet, prescribed values were input for flow velocity, activated sludge concentration, and concentrations of soluble constituents. Pressure was set to be atmospheric at the effluent outlet. No-slip boundary conditions were applied at all fixed, solid walls. The rotating equipment was simulated by the fan model and moving wall model. The water surface was treated as a rigid-lip slip wall, in order to complete the degasification process. For surface aeration referring to the rotation of the impellers, the oxygen mass transfer rate can be obtained by Equations (3) and (4).

2.3. Artificial Neural Network Model

ANNs are parallel models inspired by the biological neural networks of the human brain (Binetti et al., 2017). The calculation procedure can be separated into two stages: a forward phase during which information from input nodes is propagated forward to compute information at output nodes, and a backward stage during which connection weights are modified based on the differences between computed and observed information signals at the output nodes.

To provide sufficient data to train and validate the ANN model, 364 sets of operation conditions were calculated using the 3D three-phase model. Following the Code for Design of Outdoor Wastewater Engineering (GB50014-2006), the total coefficient of variation of the sewage treatment capacity of a general wastewater treatment plant is taken to be approximately 2.0; thus, the calculated inflow rates were 100, 125, 150 and 200 L/h. Given that the concentration of TN in the typical domestic wastewater varies from 25 to 75 mg/L and the ratio of carbon to nitrogen (C/N) ranges from 3 to 7 (Beijing general municipal engineering design & research institute, 2004), the simulated concentrations of TN were set to 25, 50 and 75 mg/L, and the C/N ratios were 3, 5 and 7. For a general OD, Hartley (2008) observed that the average concentration of sludge in the OD was 3.0 - 4.5 g/L; herein, input values of average concentration of sludge in the OD were therefore set to 3.0, 3.5, 3.9 and 4.5 g/L. The aeration rates were 1.4, 1.8, 2.2, 2.6 and 3.0 m^3/h. Reference points were located at W1, W2, W3, outlet, W4 and W5 (Figure 2) where W1 was near the starting point of the aeration zone, W2 was at the center of the aeration zone, W3 was at the end of the aeration zone, W4 and W5 were close to the start and end of the curved channel. These locations were chosen because they reflected the local hydrodynamics structures and primary water quality parameters in the aerobic and anoxic zones. Information at the six reference locations was extracted from the 3D three-phase CFD model simulations in order to train and validate the ANN model.

The constructed ANN with BP algorithm consisted of one input layer, two hidden layers, and one output layer, as shown in Figure 1. Grid input data comprised: inflow discharge, TN, C/N ratio, average sludge concentration, aeration rate, speed of impellers and stirrers, and the locations of the reference points (in terms of stream-wise distance along the inlet to each of the reference points). Grid output data consisted of the liquid velocity and the concentrations of ammonia nitrogen, nitrate, TN, DO, COD and MLSS, accounting for all the primary hydrodynamics and water quality parameters in the OD. The Levenberg-Marquardt algorithm (LMA) was implemented to train the network, noting the ability of LMA to achieve high generalization accuracy and fast convergence (Yetilmezsoy et al., 2009). The tangent sigmoid transfer function (tansig) was applied at both hidden and output layers to avoid possible undesirable, negative estimates possibly arising at the output layer. Of the 2,184 groups of data (364 sets of operation conditions), 70% were treated as the training set to cultivate the learning ability of the multi-site ANN model, and 30% were treated as the validation set to find the optimum structure with the best predictive ability (Bishop, 2006). Measurements under experimental conditions (Table 2) were treated as the test set to verify the performance of the multi-site ANN model in terms of the mean square error (MSE):

$$MSE = \frac{1}{n}\sum_{i=1}^{n}\left(x_{ci} - x_{mi}\right)^2 \tag{5}$$

and normalized standard error (OF):

$$OF = \frac{\sqrt{\frac{1}{n(n-1)}\sum_{i=1}^{n}\left(x_{ci} - x_{mi}\right)^2}}{\frac{1}{n}\sum_{i=1}^{n}x_{ci}} \tag{6}$$

where x_c and x_m represent calculated and measured value, respectively, and n is the total number of data values in each set.

To determine the effects of aeration rate and rotational speeds of the impellers and stirrers on the effluent water quality while optimizing the operation condition in the OD, the constructed multi-site ANN model was extended to predict the

Table 2. Experimental Conditions for Testing the ANN Model in the Pilot-scale Oxidation Ditch

Inflow discharge (L/h)	TN (mg/L)	Carbon-nitrogen ratio	MLSS (g/L)	Aeration rate (m^3/h)	Speed of impeller & stirrer
100	50	3	3.9	1.4	Case IV
100	50	3	3.9	1.8	Case IV
100	50	3	3.9	2.2	Case IV
100	50	3	3.9	2.6	Case IV
100	50	3	3.9	3.0	Case IV
100	50	5	3.9	1.4	Case IV
100	50	5	3.9	1.8	Case IV
100	50	5	3.9	2.2	Case IV
100	50	5	3.9	2.6	Case IV
100	50	5	3.9	3.0	Case IV
100	50	7	3.9	1.4	Case IV
100	50	7	3.9	1.8	Case IV
100	50	7	3.9	2.2	Case IV
100	50	7	3.9	2.6	Case IV
100	50	7	3.9	3.0	Case IV

concentrations of ammonia nitrogen, nitrate nitrogen, TN, and COD at the outlet. The grid inputs of the inlet condition were fixed as follows: 100L/h of inflow rate, 3.9 g/L of MLSS, 50 mg/L of NH_4^+-N and 7 of C/N. The aeration rates ranged from 1.4 to 3.0 m^3/h. The standard deviation (*Std*) of sludge was used to describe quantitatively the evenness of activated sludge in the OD, and was given by:

$$Std = \sqrt{\frac{\sum_{i=1}^{n}(MLSS_i - \overline{MLSS})^2}{n-1}} \tag{7}$$

where $MLSS_i$ is the sludge concentration at point i, $\overline{MLSS}$ is the average sludge concentration, and n is the number of points. Obviously, a lower *Std* represents a more uniform distribution of sludge.

2.4. Optimization Model Using an Accelerating Genetic Algorithm

The genetic algorithm (GA) is a global search method used to deal with complex optimization problems based on the mechanism of intra-group chromosome information exchange and survival of the fittest in the process of biological evolution (Benvidi et al., 2017; Mishra et al., 2016). GA utilizes simple coding techniques and algorithmic mechanisms, and has no restrictions on the specific form of the objective function and the number of optimization variables (Goldberg, 1969). Consequently, GA has been successfully applied in many fields (Bahrami et al., 2016; Benvidi et al., 2017; Goldberg, 1989; Weng et al., 2005). However, the standard genetic algorithm has the disadvantages of premature convergence and large computational complexity, lowing both its accuracy and computational speed (Coleman et al., 2003; Yang et al., 2005; Li et al., 2007). To overcome these shortcomings, the accelerating genetic algorithm (AGA) was developed to accelerate convergence to the optimal solution and to save computation time (Jin et al., 2000; Cai et al., 2007; Fang et al., 2009).

The AGA involves the following steps (Figure 1): determination of the initial parameters (e.g., population size, the number of smart individuals, range of variables); the encoding of variables; initialization of the parent population; calculation of the objective function and fitness value; selection; crossover; mutation; evolution; and accelerating cycles (Jin et al., 2000; Fang et al., 2009). During implementation, the processes of selection, crossover and mutation were parallelized, and the smart individuals were used to modify adaptively the search range. As a result, the AGA is faster computationally and has more opportunities to reach the global optimal solution than GA (Fang et al., 2009).

3. Results and Discussion

3.1. Simulations in Pilot-Scale Oxidation Ditch Using 3D Three-Phase CFD Model

By representing activated sludge as a pseudo-solid phase, the 3D three-phase CFD model replicated the liquid-gas-solid interactions and sludge sedimentation in OD, and good agreement was obtained between the simulated and measured liquid velocity and activated sludge concentration, with normalized standard errors of 9.6% and 2.8% (Lei et al., 2014). Likewise, the normalized standard errors between the simulated and measured ammonia nitrogen, nitrate, DO and COD concentrations were 1.5%, 3.3%, 9.9% and 1.5%, respectively, indicating that the 3D three-phase CFD model satisfactorily reproduced the key multi-phase motions and interactions in the OD. The distributions of MLSS and DO were presented in the Figure S1.

3.2. Verification of the Multi-Site ANN Model

Table 3 presents the optimum ANN structure, after training and validation, for simulations of liquid velocity, and concentrations of MLSS, ammonia nitrogen, nitrate, DO and COD at multiple sites in the OD. Using the test set to verify further the performance of the multi-site ANN model, satis-

Table 3. Optimum Structures and Test Results of the ANN Model in the Pilot-scale Oxidation Ditch

Variable	Structure	MSE	OF	R^2
Ammonia nitrogen	12−11−10−1	$7.34 * 10^{-2}$	0.33%	0.9996
Nitrate	12−8−13−1	$2.21 * 10^{-1}$	0.32%	0.9990
TN	12−14−4−1	$5.69 * 10^{-1}$	0.33%	0.9963
DO	12−7−14−1	$3.34 * 10^{-3}$	1.13%	0.9922
COD	12−12−9−1	$4.87 * 10^{-3}$	0.04%	0.9982
MLSS	12−14−13−1	$7.38 * 10^{-3}$	0.23%	0.9031
Liquid velocity	12−11−8−1	$5.26 * 10^{-5}$	1.36%	0.9822

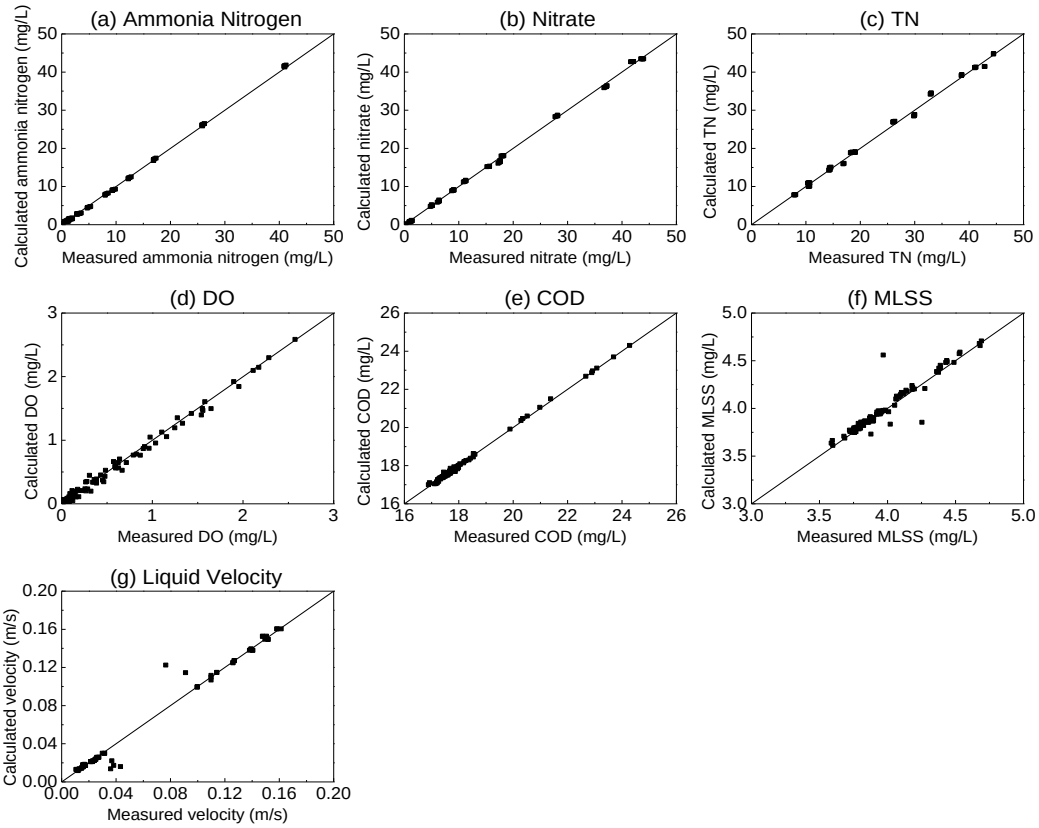

Figure 4. Comparisons between calculated and measured values of: (a) ammonia nitrogen concentration; (b) nitrate concentration; (c) TN concentration; (d) DO concentration; (e) COD concentration; (f) MLSS concentration; and (g) liquid velocity in a pilot-scale OD.

factory agreement was achieved between measured and predicted results (Figure 4 and Table 3). For all parameters considered, the correlation coefficients $R^2 > 0.9$; moreover, for ammonia nitrogen, nitrate, TN, DO and COD, $R^2 > 0.99$. In all cases, MSE < 0.6 (between measured and the simulated results), and the normalized standard errors of the liquid velocity, MLSS, ammonia nitrogen, nitrate, TN, DO and COD concentrations were 1.36, 0.23, 0.33, 0.32, 0.33, 1.13 and 0.04%, respectively. Therefore, the multi-site ANN model proved highly capable of predicting the local hydrodynamics, deposition of activated sludge, and water quality indexes at multiple locations in the OD.

3.3. Improved Simulation Time

All the simulations were performed on a workstation equipped with two Intel Xeon 2.93 GHz processors and 24 GB RAM. For the 3D three-phase model, 24 hours of CPU time were required to reach steady state in each case considered (Lei et al., 2014). By comparison, the multi-site ANN model trained using the 3D three-phase model required only 1 s of CPU time to calculate the same operational mode case. The trained multi-site ANN model was 86,400 times faster to run than the 3D three-phase CFD model on its own, a 99.99% total time saving.

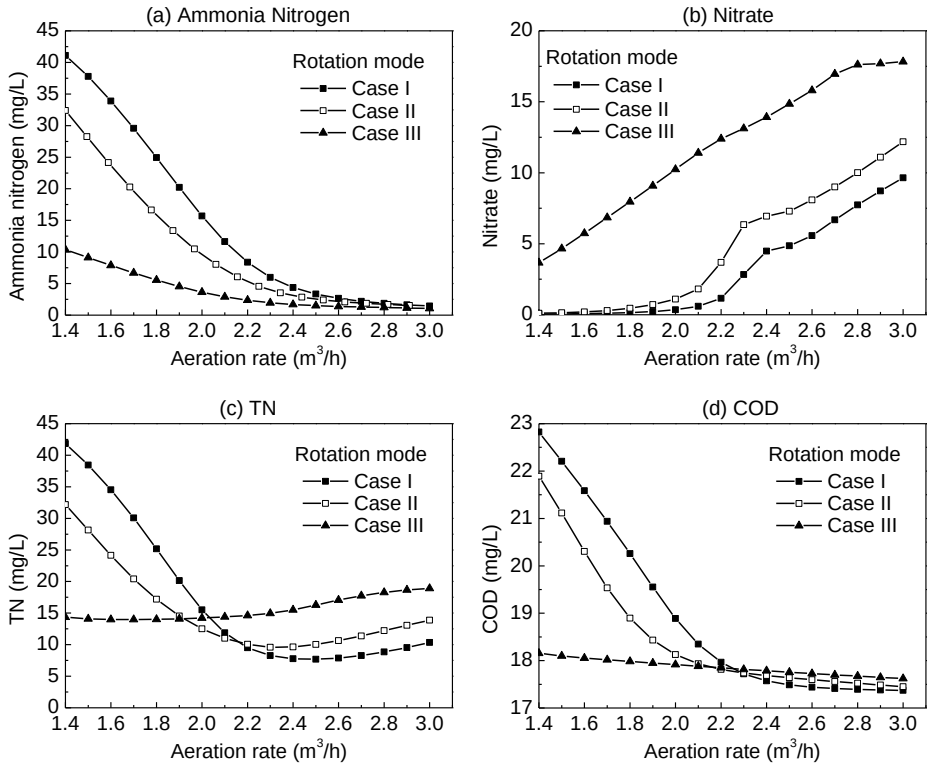

Figure 5. Predicted effluent concentrations of (a) ammonia nitrogen, (b) nitrate, (c) TN, and (d) COD as functions of aeration rate, at an elevation 0.25 m above the bottom of the pilot-scale OD under three different operation modes.

Table 4. Optimized Operating Condition in the Pilot-scale OD

Operation condition							Effluent quality					V^9	E^{10}
x^1	a^2_1	a_2	b^3_1	b_2	b_3	b_4	NH^4	NO^5	TN^6	DO^7	COD^8		
1.60	46.35	43.02	47.06	55.73	78.67	88.76	4.36	0.14	4.50	0.01	25.0336	0.07	216.90

x^1: aeration rate, m^3/h; a^2: rotating speed of impeller, rpm; b^3: rotating speed of stirrer, rpm; NH^4: concentration of ammonia nitrogen, mg/L; NO^5: concentration of nitrate, mg/L; TN^6: concentration of total nitrogen, mg/L; DO^7: concentration of dissolved oxygen, mg/L; COD^8: concentration of COD, mg/L;V^9: averaged liquid velocity, m/s; E^{10}: energy consumption, W.

3.4. Effect of Aeration Rate and Rotational Speed on Effluent Water Quality

On the one hand, as the aeration rate and rotational speed increased, the effluent concentrations of ammonia nitrogen (Figure 5a) and COD (Figure 5d) decreased asymptotically to almost zero and 17.5 mg/L respectively, because of enhanced nitrification in the aerobic zones at the higher DO levels, thereby increasing the removal efficiency of inlet ammonia nitrogen and COD. On the other hand, the increased aeration rate and rotational speed caused the steep rise of nitrate concentration in the effluent (Figure 5b) owing to progressive accumulation from active nitrification and reducing consumption by inhibited denitrification at high averaged DO concentration. Consequently, the effluent TN concentration, given by the sum of ammonia nitrogen and nitrate, initially declined, reached a minimum, and then increased as the aeration rate and rotational speed increased (Figure 5c). It should be noted that the lowest concentration of TN did not occur at the highest aeration rate or rotational speed; in practice, it would be necessary to commence from intermediate aeration rates and rotational speeds and then control them jointly to ensure the highest effluent efficiency is achieved.

3.5. Optimization in Pilot-Scale Oxidation Ditch

According to the Discharge Standards of Pollutants for Municipal Wastewater Treatment Plant (GB 18918-2002), the effluent concentrations of COD, ammonia nitrogen, and TN must be lower than 50 mg/L, 5 mg/L and 15 mg/L, respectively, for treated effluent to reach the first-class A level. The critical velocity to ensure an even deposition of sludge was determined as 0.06 m/s (Figure S2). Within the application ranges of the aerator, surface impeller, and submerged stirrer, the constraints are expressed as:

$$COD_{out} < 50\ mg/L \quad (8)$$

$$NH_4^+ - N_{out} < 5\ mg/L \quad (9)$$

$$TN_{out} < 15\ mg/L \quad (10)$$

$$\bar{v} > 0.06\ m/s \quad (11)$$

$$1.4\ m^3/h \le Air \le 3\ m^3/h \quad (12)$$

$$40\ rpm \le Impeller(i) \le 180\ rpm \quad (13)$$

$$40\ rpm \le Stirrer(j) \le 120\ rpm \quad (14)$$

where COD_{out}, NH_4^+ - N_{out}, and TN_{out} are the effluent concentrations of COD, ammonia nitrogen and TN, respectively; *Air* represents the aeration rate; $Impeller(i)$ is the rotational speed of the *i*-th surface impeller; and $Stirrer(j)$ is the rotational speed of the *j*-th submerged stirrer. The objective function could be expressed:

$$E_{\min} = \min E \quad (15)$$

where *E* represents energy consumption. The energy consumption of each component used in the OD was measured by a power meter socket (LINI-T UT230C); Figure S3 presents curves of energy consumption against aeration rate, rotational speed of surface impeller, and rotation speed of submerged stirrer.

Before using AGA to optimize the operating conditions in the OD, all key parameters, including the population size, number of smart individuals and generation number, must be determined. Different population sizes were used to build the AGA model, as shown in Figure S4a. During the first 20 generations, the energy consumption decreased largely overall, with relatively small fluctuation. Energy consumption remained stable after 50 generations, and so the generation number was set to 50. Figure S4a also shows that a small population size could not produce all the important information and readily lead to a local optimum. However, a large population size resulted in increased computation and low efficiency. Hence, the population size was prescribed to be 500. In Figure S4b, the population size was kept fixed at 500, while different numbers of smart individuals were calculated. A larger number of smart individuals resulted in a low convergence rate because the intervals of the variables changed slowly. However, fewer smart individuals would lead to local optima because of information loss. Thus, the number of smart individual was set to 30.

Table 4 lists the optimization results obtained by AGA. The lowest energy consumption is 216.90 W, which met the first-class A level of effluent quality standards in China while achieving an even deposition of sludge.

4. Applications to Full-Scale OD

4.1. Full-Scale OD at Ping Dingshan WWTP, China

The full-scale bioreactor at the Ping Dingshan WWTP, Henan Province, China, was a four-channel circular ditch with a total working volume of 26,000 m^3, and the wastewater flow rate of 50000 m^3/d. Each straight channel was 130 m long, 10 m wide, and had a mean water depth of 4 m (Figure 6). The larger semi-circular connecting channel at the right-hand end of the straight channel had a center-line radius of 20.4 m. Each of the smaller semi-circular channels had a center-line radius of 10.15 m. The OD contained a total of 13 sets of surface aerators and 9 sets of submerged impellers (Figure 6), not all of which were necessarily operated at any one time. Each set of aerators consisted of 45 discs; and each disc was 10 m long (about 0.5 m of which was submerged) and 1.4 m in diameter with rotational speed of 53 rpm. Each surface aerator provided an oxygenation mass addition rate of 65 kgO_2/h and required a power input of 37 kW. And each single submerged impeller had two 2.0 m diameter blades, and required a power input of 4.19 kW. The submerged impellers were installed 2.2 m below the liquid free surface, and when running, the wastewater mixture could be accelerated through the impellers. Under existing operating conditions, a total of 9 surface aerators and 3 submerged impellers operated simultaneously (Figure 6). Table S1 summarizes the characteristics of the influent and effluent water quality indexes under existing operating conditions. The designed averaged concentration of sludge was 4.0 g/L, and the sludge retention time was 15 d. The hydraulic retention time was 12.48 h, of which the wastewater spent 9.98 h in aerobic zones occupying 20,800 m^3 working volume and 2.50 h in anoxic zones of 5,200 m^3 working volume. Throughout operation of the OD, the wastewater temperature was 18.2 - 25.5 °C, and the pH was approximately 7.4.

Horizontal flow velocity components in the straight and semicircle portions were measured using an XZ-3 probe (an intelligent current meter; manufactured by Nanjing Automation Institute of Water Resources and Hydrology, Ministry of Water Resources of China). On-line DO measurements were acquired using an Endress + Hauser meter (made in Germany). In order to reflect the local hydrodynamics structures and to determine primary water quality parameters at different depths, measurements were made at three streamwise locations and at four different depths: 3.5 m from the bottom (Surface Layer), 3 m from the bottom (Top Layer), 2 m from the bottom (Middle Layer), and 1 m from the bottom (Bottom Layer) of the ditch (Yang et al., 2011) (Figure S5). The flow speed near the dich bottom is usually small, especially in the anoxic zone and the corner. Therefore, if the bottom layer is set much closer to the ditch bottom, the flow speed will be much lower and difficult to monitor that ultimately affects the measurement accuracy.

4.2. Development of Hybrid Model

In the 3D three-phase CFD model used to simulate the full-scale OD, the open boundary conditions were set at the

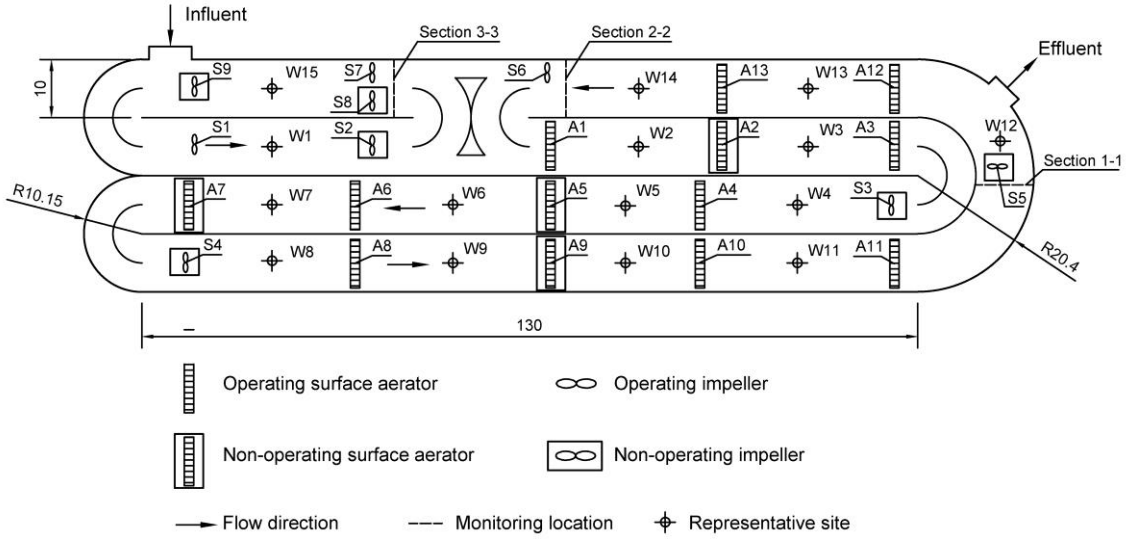

Figure 6. Full-scale oxidation ditch in the existing operating condition and representative sites, Ping Dingshan, Henan Province, China (Unit: m).

inlet and outlet of the ditch. The prescribed influent flow velocity, activated sludge concentration, and concentrations of soluble constituents were applied at the inlet boundary and atmospheric pressure at the outlet boundary. A rigid-lid approximation was applied at the water surface, and a no-slip boundary condition was assigned to all fixed walls. Rotating devices were simulated by the fan model and the moving wall model. The wall roughness height was set as 0.02 m, and the roughness constant was 1 (Yang et al., 2011). All other parameters used in this simulation were chosen to be the same as those in the pilot-scale OD simulation (Lei et al., 2014).

Figure S6 presents a comparison of predicted and measured liquid velocity at Sections 1-1, 2-2 and 3-3 under existing operating conditions; reasonable agreement is evident, as indicated by the normalized standard error of 5.3%. The larger simulation error of liquid velocity in the surface layer is mainly caused by the assumption of rigid-lip slip wall in the water surface and the existence of surface disturbance in the full-scale WWTP. Figure S7 presents the color contours of magnitude of horizontal velocity components; the visualization shows the presence of an uneven flow pattern under existing operating conditions in the oxidation ditch; in particular, the horizontal flow speed near an internal wall is usually lower than that near the corresponding external wall. Figure S8 shows that the predicted DO concentration profiles are in reasonable agreement with their measured counterparts at transects in the aerobic zone (Section 2-2) and anoxic zone (Section 3-3), with a normalized standard error of 2.6%. The simulation errors on DO concentration profiles were slightly greater in the surface and top layers than those in other layers. This is mainly because of the complexity of oxygen mass transfer phenomenon in the OD and the simplification of degasification process. Table S2 lists the corresponding measured and calculated effluent concentrations of COD, ammonia nitrogen, and TN, with normalized standard errors of 9.2 %, 15.0 % and 8.6 %, respectively. These validation results established that the CFD model accurately reflected the characteristics of liquid velocity, DO profiles and effluent quality in the full-scale OD.

The calibrated 3D three-phase CFD model was then used to simulate a total of 260 groups of operational modes, and the results transferred as node inputs to the ANN model. The input data were randomly divided into training, validation, and test sets. Fourfold cross validation was used to limit the bias caused by random selection of training set. Node outputs comprised estimates of concentrations of ammonia nitrogen, nitrate, TN, and COD, and the liquid velocity in the OD. The training algorithm was LMA, and tansig was used as the transfer function in both the hidden and output layers. Table 5 presents the optimum ANN structure used for simulating average liquid velocity and effluent water quality indexes; the high values of correlation coefficient demonstrate the close match between the CFD and ANN predictions. Importantly, the CPU time reduced from 32 h using CFD to 1.2 s using ANN for the same operation mode.

The aim is to achieve low operating costs, a relatively even distribution of activated sludge, and first-class A level effluent water quality. To achieve this, the correlation between average liquid velocity and *Std* of MLSS was determined at reference locations along the OD, each an elevation 0.5 m above the bed of the ditch, for all operation modes considered (Figure S9). It was thus found that the critical velocity required to achieve an even distribution of sludge was 0.15 m/s. Based on Yang et al.'s study (Yang et al., 2011), 6 surface aerators were needed to meet the oxygen demand requirements in the Ping Dingshan OD. Moreover, the effluent concentrations of COD, ammonia nitrogen, and TN must be lower than 50 mg/L, 5 mg/L and 15 mg/L, respectively, for treated effluent

Table 5. Optimum Structures and Test Results of the ANN Model in the Full-scale Oxidation Ditch, Ping Dingshan, Henan Province, China

Variable	Structure	MSE	RSD	R^2	BLE
Ammonia nitrogen	23-15-13-1	0.2701	0.17%	0.9864	y = 0.9973x + 0.0571
Nitrate	23-14-4-1	0.1570	0.59%	0.9523	y = 0.9602x + 0.085
TN	23-14-9-1	0.3416	0.14%	0.9704	y = 0.9952x + 0.0709
COD	23-12-2-1	2.4733	0.21%	0.9886	y = 0.9786x + 0.5775
Liquid velocity	23-7-8-1	0.0004	0.60%	0.9216	y = 0.9421x + 0.0078

* R^2: Correlation coefficient; BLE: Best linear fitting equation.

Table 6. Optimized Operating Condition in Full-Scale OD, Ping Dingshan, Henan Province, China

Number	Surface aeration												
	A1	A2	A3	A4	A5	A6	A7	A8	A9	A10	A11	A12	A13
1	0^1	1^2	0	1	0	1	0	1	0	1	0	0	1
2	0	1	0	1	0	1	0	1	0	1	0	0	1
3	0	1	0	1	0	1	0	1	0	1	0	1	0
4	1	0	0	1	0	1	0	1	0	1	0	0	1
5	1	0	0	1	0	1	0	1	0	1	0	1	0

* 0^1: Non-operation; 1^2: Operation.

Table 7. Optimized Operating Condition in Full-Scale OD, Ping Dingshan, Henan Province, China

Number	Submerged impeller									Effluent quality				V^7	E^8
	S1	S2	S3	S4	S5	S6	S7	S8	S9	NH^3	NO^4	TN^5	COD^6		
1	0	0	1	0	1	1	0	0	1	4.76	9.08	13.84	30.19	0.16	238.76
2	1	0	1	0	1	0	0	0	1	4.12	3.39	7.51	30.04	0.16	238.76
3	0	0	1	0	1	0	1	0	1	4.43	2.46	6.89	28.65	0.16	238.76
4	1	0	1	0	1	0	0	0	1	4.89	4.64	9.53	29.96	0.16	238.76
5	0	0	1	0	1	0	1	0	1	2.48	4.01	6.49	29.76	0.16	238.76

* NH^3: concentration of ammonia nitrogen, mg/L; NO^3: concentration of nitrate, mg/L; TN^5: concentration of total nitrogen, mg/L; COD^6: concentration of COD, mg/L; V^7: averaged liquid velocity, m/s; E^8: energy consumption, kW.

to reach the first-class A level. Similarly, the objective function could be expressed as Equation (15).

The population size of the AGA was set to 300, the number of smart individuals was 20, and the generation number was 100. Tables 6 and 7 list the five best sets of results. Here, the effluent TN concentration has reduced from 19.7 mg/L (existing condition) to less than 14 mg/L (Table 6), meeting the effluent quality standards of first-class A level. Compared with 345.57 kWh energy consumption under existing conditions, the improved conditions saved 106.81 kWh (31%) of the energy, resulting in a cost saving of about 65,000 € per annum, assuming a tariff of 0.07 €/kWh (Vanrolleghem et al., 2001).

5. Conclusions

Oxidation ditches involve complicated interacting physical-chemical-biological processes, and need system optimization to meet water quality standards, sludge deposition requirements, and economic constraints. Rapid feedback control and real-time optimization are therefore urgently required for many WWTPs. The proposed hybrid model inherited the advantages of the 3D three-phase CFD model for simulation of the key liquid-sludge-gas motions and interactions and those of multi-site ANN models for rapid feedback, and thereby allowed real-time prediction of liquid flow velocity, MLSS concentration and major constituents. When applied to the pilot-scale OD, the hybrid model led to a speed up in computational speed that was 86,400 times faster than CFD simulations would have cost. Furthermore, the introduced AGA model enhanced system optimization, which demonstrated a 31% saving in total energy compared to the existing operating condition in a full-scale OD. The hybrid model presented herein is potentially very useful in providing rapid prediction in the ODs, and in helping achieve real-time process optimization control in practice.

Acknowledgments. Financial support from the National Natural Science Foundation of China (Grant No. 51539001) is very much appreciated.

Supporting Material: This paper contains supporting materials which are available in its online version.

References

Aguado, D., Ribes, J., Montoya, T., Ferrer, J. and Seco, A. (2009). A methodology for sequencing batch reactor identification with artificial neural networks: A case study. *Comput. Chem. Eng*., 33(2), 465-472. https://doi.org/10.1016/j.compchemeng.2008.10.018

Bahrami, S., Ardejani, F.D., and Baafi, E. (2016). Application of artificial neural network coupled with genetic algorithm and simulated annealing to solve groundwater inflow problem to an advancing open pit mine. *J. Hydrol*., 536, 471-484. https://doi.org/10.1016/j.jhydrol.2016.03.002

Benvidi, A., Abbasi, S., Gharaghani, S., Tezerjani, M.D., and Masoum, S. (2017). Spectrophotometric determination of synthetic colorants using PSO-GA-ANN. *Food Chem*., 220(1), 377-384. https://doi.org/10.1016/j.foodchem.2016.10.010

BGMEDRI (Beijing General Municipal Engineering Design & Research Institute). (2004). Water Supply and Drainage Design Manual (in Chinese), *China Building Industry Press*, China.

Binetti, G., Coco, L.D., Ragone, R., Zelasco, S., Perri, E., Montemurro, C., Valentini, R., Naso, D., Fanizzi, F.P., and Schena, F.P. (2017). Cultivar classification of Apulian olive oils: Use of artificial neural networks for comparing NMR, NIR and merceological data. *Food Chem*., 219, 131-138. https://doi.org/10.1016/j.foodchem.2016.09.041

Bishop, C.M. (2006). Pattern Recognition and Machine Learning, Springer.

Cai, Y., Huang, G. H., Nie, X. H., Li, Y. P., and Tan, Q. (2007). Municipal solid waste management under uncertainty: a mixed interval parameter fuzzy-stochastic robust programming approach. *Environ. Eng. Sci*., 24(3), 338-352. https://doi.org/10.1089/ees.2005.0140

Çinar, Ö., Hasar, H., and Kinaci, C. (2006). Modeling of submerged membrane bioreactor treating cheese whey wastewater by artificial neural network, *J. Biotechnol*., 123(2), 204-209. https://doi.org/10.1016/j.jbiotec.2005.11.002

Coleman, M.C., Buck, K.K.S., and Block, D.E. (2003). An integrated approach to optimization of Escherichia coli fermentations using historical data. *Biotechnol. Bioeng*., 84(3), 274-285. https://doi.org/10.1002/bit.10719

EPA. (1992). *Evaluation of Oxidation Ditches for Nutrient Removal*, Washington, United States Environmental Protection Agency.

Fang, F., Ni, B.J., and Yu, H.Q. (2009). Estimating the kinetic parameters of activated sludge storage using weighted non-linear least-squares and accelerating genetic algorithm. *Water Res*., 43(10), 2595-2604. https://doi.org/10.1016/j.watres.2009.01.002

Fernando, H., and Surgenor, B. (2017). An unsupervised artificial neural network versus a rule-based approach for fault detection and identification in an automated assembly machine. *Robot. Comput. Integr. Manuf*., 43, 79-88. https://doi.org/10.1016/j.rcim.2015.11.006

Glover, G.C., Printemps, C., Essemiani, K., and Meinhold, J. (2006). Modelling of wastewater treatment plants - how far shall we go with sophisticated modelling tools? *Water Sci. Technol*., 53(3), 79-89. https://doi.org/10.2166/wst.2006.078

Goldberg, D.E. (1989). *Genetic Algorithms in Search*, Optimization and Machine Learning, Addison-Wesley.

Häck, M., and Köhne, M. (1996). Estimation of wastewater process parameters using neural networks. *Water Sci. Technol*., 33(1), 101-115. https://doi.org/10.1016/0273-1223(96)00163-1

Hartley, K.J. (2008). Controlling sludge settleability in the oxidation ditch process. *Water Res*., 42(6-7), 1459-1466. https://doi.org/10.1016/j.watres.2007.10.017

He, L., Ji, F.Y., Zhou, W.W., Xu, X., Chen, R.H., Liu, N., and He, X.L. (2014). Deposition pattern, effect on nitrogen removal and component analysis of deposited sludge in a carrousel oxidation ditch. *Desalination Water Treat*., 52(31-33), 6079-6087. https://doi.org/10.1080/19443994.2013.815582

Henze, M., Gujer, W., Mino, T., and van Loosdrecht, M. (2000). Activated Sludge Models ASM1, ASM2, ASM2d and ASM3, IWA.

Holenda, B., Domokos, E., Rédey, Á., and Fazakas, J. (2008). Dissolved oxygen control of the activated sludge wastewater treatment process using model predictive control. *Comput. Chem. Eng*., 32(6), 1270-1278. https://doi.org/10.1016/j.compchemeng.2007.06.008

Jin, J.L., Yang, X.H., and Ding, J. (2000). Real coding based acceleration genetic algorithm. *J. Sichuan Univ*., 32, 20-24.

Jin, P.K., Wang, X.B., Wang, X.C., Ngo, H.H., and Jin, X. (2015). A new step aeration approach towards the improvement of nitrogen removal in a full scale Carrousel oxidation ditch. *Bioresour. Technol*., 198, 23-30. https://doi.org/10.1016/j.biortech.2015.08.145

Karpinska, A.M., and Bridgeman, J. (2016). CFD-aided modelling of activated sludge systems - A critical review. *Water Res*., 88(1), 861-879. https://doi.org/10.1016/j.watres.2015.11.008

Lei, L., and Ni, J.R. (2014). Three-dimensional three-phase model for simulation of hydrodynamics, oxygen mass transfer, carbon oxidation, nitrification and denitrification in an oxidation ditch. *Water Res*., 53, 200-214. https://doi.org/10.1016/j.watres.2014.01.021

Li, Y. P., Huang, G. H., and Nie, S. L. (2007). Mixed interval–fuzzy two-stage integer programming and its application to flood-diversion planning. *Eng. Optimiz*., 39(2), 163-183. https://doi.org/10.1080/03052150601044831

Littleton, H.X., Daigger, G.T., and Strom, P.F. (2007). Application of computational fluid dynamics to closed-loop bioreactors: II. Simulation of biological phosphorus removal using computational fluid dynamics. *Water Environ. Res*., 79, 613-624. https://doi.org/10.2175/106143006X136748

Ma, Y.W., Huang, M.Z., Wan, J.Q., Wang, Y., Sun, X.F., and Zhang, H.P. (2011). Prediction model of DnBP degradation based on BP neural network in AAO system. *Bioresour. Technol*., 102(6), 4410-4415. https://doi.org/10.1016/j.biortech.2011.01.004

Mishra, A.K., Kumar, B., and Dutta, J. (2016). Prediction of hydraulic conductivity of soil bentonite mixture using hybrid-ANN approach. *J. Environ. Inf*., 27(2), 98-105. https://doi.org/10.3808/jei.201500292

Pipes, W.O. (1969). Types of activated sludge which separate poorly. *J. Water Pollut. Control Fed*., 41, 714-724.

Purkait, B., Kadam, S.S., and Das, S.K. (2008). Application of artificial neural network model to study arsenic contamination in groundwater of Malda District, Eastern India. *J. Environ. Inf*., 12(2), 140-149. https://doi.org/10.3808/jei.200800132

Shen, W.H., Chen, X.Q., and Corriou, J.P. (2008). Application of model predictive control to the BSM1 benchmark of wastewater treatment process. *Comput. Chem. Eng*., 32(12), 2849-2856. https://doi.org/10.1016/j.compchemeng.2008.01.009

Stare, A., Vrečko, D., Hvala, N., and Strmčnik, S. (2007). Comparison of control strategies for nitrogen removal in an activated sludge process in terms of operating costs: A simulation study. *Water Res*., 41(9), 2004-2014. https://doi.org/10.1016/j.watres.2007.01.029

Vanrolleghem, P., and Gillot, S. (2001). Robustness and economic measures as control benchmark performance criteria. *Water Sci. Technol*., 45, 117-126.

Wei, W.L., Zhang, Z.W., Zheng, Y., and Liu, Y.L. (2016b). Numerical simulation of additional guiding baffles to improve velocity distribution in an oxidation ditch. *Desalination Water Treat*., 57(51),

24257-24266. https://doi.org/10.1080/19443994.2016.1141373

Weng, H.T., and Liaw, S.L. (2005). Establishing an optimization model for sewer system layout with applied genetic algorithm. *J. Environ. Inf*., 5(1), 26-35. https://doi.org/10.3808/jei.200500043

Yang, X.H., Yang, Z.F., and Shen, Z.Y. (2005). GHHAGA for environmental systems optimization. *J. Environ. Inf*., 5(1), 36-41. https://doi.org/10.3808/jei.200500044

Yang, Y., Yang, J.K., Zuo, J.L., Li, Y., He, S., Yang, X., and Zhang, K. (2011). Study on two operating conditions of a full-scale oxidation ditch for optimization of energy consumption and effluent quality by using CFD model. *Water Res*., 45(11), 3439-3452. https://doi.org/10.1016/j.watres.2011.04.007

Yetilmezsoy, K., and Sapci-Zengin, Z. (2009). Stochastic modeling applications for the prediction of COD removal efficiency of UASB reactors treating diluted real cotton textile wastewater. *Stochastic Environ. Res. Risk Assess*., 23, 13-26.

Zeng, G.M., Qin, X.S., He, L., Huang, G.H., Liu, H.L., and Lin, Y.P. (2003). A neural network predictive control system for paper mill wastewater treatment. *Eng. Appl. Artif. Intell*., 16(2), 121-129. https://doi.org/10.1016/S0952-1976(03)00058-7

Zhang, Q.H., Yang, W.N., Ngo, H.H., Guo, W.S., Jin, P.K., Dzakpasu, M., Yang, S.J., Wang, Q., Wang, X.C., and Ao, D. (2016). Current status of urban wastewater treatment plants in China. *Environ. Int*., 92-93, 11-22. https://doi.org/10.1016/j.envint.2016.03.024

Zhou, X., Han, Y.P., and Guo, X.S. (2015). Identification and evaluation of SND in a full-scale multi-channel oxidation ditch system under different aeration modes. *Chem. Eng. J*., 259, 715-723. https://doi.org/10.1016/j.cej.2014.07.133